

Influence of Secondary Structure on the Fragmentation of Protonated Peptides

George Tsapraillis,[†] Hari Nair,[†] Árpád Somogyi,[†] Vicki H. Wysocki,^{*,†} Wenqing Zhong,[‡] Jean H. Futrell,[‡] Scott G. Summerfield,[§] and Simon J. Gaskell[§]

Contribution from the Departments of Chemistry, University of Arizona, P.O. Box 210041, Tucson, Arizona 85721-0041, and University of Delaware, Newark, Delaware 19716, and The Michael Barber Center for Mass Spectrometry, UMIST, P.O. Box 88, Manchester M69 1QD, U.K.

Received August 19, 1998

Abstract: The influence of acid–base interactions on the gas-phase dissociation of a series of protonated peptides was investigated. Peptides containing both acidic residues [aspartic (D), glutamic (E), and cysteic acid (C*)] and basic residues [arginine (R)] were dissociated by different activation methods that allow different time frames for dissociation. The synthetic peptides investigated differ systematically in the number and position of arginine residue(s) and include *RLDIFSDFR*, *RLEIFSEFR*, *RLDIFSDF*, *LDIFSDFR*, *LEIFSEFR*, *LDIFSDF*, *RLCIFSCFR*, *RLAIFSCFR*, *RLCIFSAFR*, *RLC*IFSC*FR*, *RLAIFSC*FR*, and *RLC*IFSFAFR* (where C* denotes cysteic acid). It was observed that the number of ionizing protons relative to the number of basic residues in peptides containing acidic residues is a contributing factor in the fragmentation behavior. Nonselective cleavages along the peptide backbone occur when the number of ionizing protons exceeds the number of arginine residues, while dominant cleavages adjacent to the acidic residues predominate when the number of ionizing protons equals the number of arginine residues. In particular, enhanced b_7/y_2 , and y_6, y_2 singly charged fragment ions were detected for the doubly protonated *RLDIFSDFR* and singly protonated *LDIFSDFR* precursor ions, respectively. These are the result of enhanced cleavage of the DF bond in the doubly protonated *RLDIFSDFR* and the DI plus DF bonds in the singly protonated *LDIFSDFR*. Abundant d and b-H₂SO₃ product ions indicative of specific cleavages adjacent to C* were observed in the cysteic acid-containing peptides when the number of ionizing protons equaled the number of arginine residues. Dominant cleavages at glutamic acid(s) were also observed for doubly protonated *RLEIFSEFR* and singly protonated *LEIFSEFR* when longer dissociation times were available. Preferential cleavage(s) at the acidic residue(s) occurs on the microsecond time scale for aspartic acid and greater than microsecond time scale for glutamic acid. This different behavior for aspartic vs glutamic acid is likely to have important implications in mass spectrometry-based sequencing strategies. However, the product ion spectra of most of the peptides investigated (*RLDIFSDFR*, *RLDIFSDF*, *LDIFSDFR*, *LEIFSEFR*, and *LDIFSDF*) were found to be very similar under the array of activation methods used. These included surface-induced dissociation in a quadrupole tandem mass spectrometer, high-energy collision-induced dissociation in a hybrid sector/time-of flight mass spectrometer, and sustained off-resonance irradiation in a Fourier transform mass spectrometer. The unique fragmentation of peptides containing basic and acidic residues is rationalized as evidence for the existence of gas-phase intramolecular solvation that strongly influences their fragmentation. We propose that it is the available acidic proton(s) on the acidic residue(s) not involved in solvating the protonated arginine that is initiating the dominant cleavage(s). Electrospray ionization/SID fragmentation efficiency curves (percent fragmentation versus laboratory collision energy) are also presented for these peptides. The positions of the curves for the doubly protonated, double arginine-containing peptides (*RLDIFSDFR*, *RLEIFSEFR*) relative to those for the doubly protonated but single arginine-containing peptides (*LDIFSDFR*, *RLDIFSDF*) are consistent with localization of charge at the two R side chains in the former peptides and formation of a heterogeneous population of protonated peptides in the latter peptides. These curve positions and the nonselective fragmentation in the peptide devoid of arginine residues (*LDIFSDF*) are consistent with the mobile proton model, which relates ease of fragmentation to ease of nonselective intramolecular proton transfer within the protonated peptides.

Introduction

Interaction between acidic and basic amino acid residues is a common structural feature for peptides/proteins in solution.

* To whom correspondence should be addressed. E-mail: vwysoc@u.arizona.edu.

[†] University of Arizona.

[‡] University of Delaware.

[§] The Michael Barber Center for Mass Spectrometry, UMIST.

These interactions are often characterized by techniques such as NMR¹ and X-ray crystallography.² The nature of similar interactions for protonated peptides and proteins in the gas phase has not been fully characterized, although indirect evidence for

(1) Dyson, H. J.; Wright, D. E. *Annu. Rev. Biophys. Chem.* **1991**, *20*, 519–538.

(2) Diffraction Methods for Biological Macromolecules. *Methods Enzymol.* **1985**, *114* and *115* (special issues).

their existence is emerging.^{3–15} This comes at a time when protein chemistry studies, traditionally reserved to the solution phase, are expanding at a rapid rate into the gas phase. These gas-phase studies, which have involved investigations ranging from studying protein folding to mapping protein function,¹⁶ are possible because of the development of “soft” ionization methods such as matrix-assisted laser desorption (MALDI)¹⁷ and electrospray ionization (ESI),^{18–20} which allow formation of singly or multiply protonated peptides and proteins. One area of interest is the relationship of structural features of proteins and peptides in solution to those in the absence of solvent (e.g., secondary, tertiary, quaternary structure as well as inter- and intramolecular solvation effects on structure). Nonetheless, some chemists argue that gas-phase structures of biomolecules are of limited interest because the gas phase is not the native environment of biomolecules. The drive to stabilize or “bury” charge in the gas phase, with no external solvent molecules present, surely leads to some differences between solution and gas-phase higher order structure. However, some structural features may be the same in solution and in the gas phase, and investigations that prove this correspondence will increase our understanding of the role (or lack of role) of solvent in aspects of protein folding. Gas-phase studies are also beginning to evolve to include controlled numbers of solvent molecules.²¹ For the work described below, the gas-phase structures are of great interest because *gas-phase secondary structure can influence dissociation patterns of energized protonated mol-*

ecules, and thus determination of primary sequence by tandem mass spectrometry (MS/MS).

Tandem mass spectrometry,²¹ coupled with sequence searches of protein and nucleotide databases,^{22–24} is used routinely as a means of structure determination of peptides and proteins^{23–43} and involves activation and subsequent fragmentation of selected protonated peptides. In fact, MS/MS sequencing of peptides is becoming the method of choice, especially for modified peptides (including N-terminal blocked peptides) and complex mixtures, where classical Edman sequencing methods are incompatible.³ For protein characterization, MS/MS spectra are acquired for several of the peptides of a digest. Peptide fragment ions result from cleavages along the peptide backbone⁴⁴ and/or the various amino acid side chains. Cleavage of the amide bond with retention of the charge on the C-terminal peptide fragment results in y_n ions, whereas if the charge is retained on the N-terminal side, b_n ions are generated.^{26–29,31} Ions 28 u lower

(3) Buret, O.; Yang, C.-Y.; Gaskell, S. J. *J. Am. Soc. Mass Spectrom.* **1992**, *3*, 337–344.

(4) Gonzalez, J.; Besada, V.; Garay, H.; Reyes, O.; Padron, G.; Tambara, Y.; Takao, T.; Shimonishi, Y. *J. Mass Spectrom.* **1996**, *31*, 150–158.

(5) Summerfield, S. G.; Whiting, A.; Gaskell, S. J. *Int. J. Mass Spectrom. Ion Processes* **1997**, *162*, 149–161.

(6) Schnier, P. D.; Price, W. D.; Jockusch, R. A.; Williams, E. R. *J. Am. Chem. Soc.* **1996**, *118*, 7178–7189.

(7) Wyttenbach, T.; von Helden, G.; Bowers, M. T. *J. Am. Chem. Soc.* **1996**, *118*, 8355–8364. (b) Wyttenbach, T.; Bushnell, J. E.; Bowers, M. T. *J. Am. Chem. Soc.* **1998**, *120*, 5098–5103.

(8) Vachet, R. W.; Asam, M. R.; Glish, G. L. *J. Am. Chem. Soc.* **1996**, *118*, 6252–6256.

(9) Buret, O.; Orkiszewski, R. S.; Ballard, K. D.; Gaskell, S. J. *Rapid Commun. Mass Spectrom.* **1992**, *6*, 658–662.

(10) Price, W. D.; Jockusch, R. A.; Williams, E. R. *J. Am. Chem. Soc.* **1997**, *119*, 11988–11989.

(11) Price, W. D.; Schnier, P. D.; Jockusch, R. A.; Strittmatter, E. F.; Williams, E. R. *J. Am. Chem. Soc.* **1996**, *118*, 10640–10644.

(12) (a) Gross, D. S.; Williams, E. R. *J. Am. Chem. Soc.* **1995**, *117*, 883–890. (b) Campbell, S.; Rodgers, M. T.; Marzluff, E. M.; Beauchamp, J. L. *J. Am. Chem. Soc.* **1995**, *117*, 12840–12854. (c) Grese, R. P.; Cerny, R. L.; Gross, M. L. *J. Am. Chem. Soc.* **1989**, *111*, 2835–2842.

(13) Lee, S.-W.; Kim, H. S.; Beauchamp, J. L. *J. Am. Chem. Soc.* **1998**, *120*, 3188–3195.

(14) Barril, X.; Aleman, C.; Orozco, M.; Luque, F. J. *Proteins Struct. Funct. Genet.* **1998**, *32*, 67–79.

(15) Melo, A.; Ramos, M. J. *Chem. Phys. Lett.* **1995**, *245*, 498–502.

(16) Winston, R. L.; Fitzgerald, M. C. *Mass Spectrom. Rev.* **1997**, *16*, 165–179.

(17) (a) Karas, M.; Bachma, U.; Hillenkamp, F. *Int. J. Mass Spectrom. Ion Processes* **1987**, *78*, 53–81. (b) Hillenkamp, F.; Karas, M.; Beavis, R. C.; Chait, B. T. *Anal. Chem.* **1991**, *63*, 1193A–1203A.

(18) (a) Dole, M.; Mack, L. L.; Hines, R. L.; Mobley, R. C.; Ferguson, L. D.; Alice, M. B. *J. Chem. Phys.* **1968**, *49*, 2240–2249. (b) Fenn, J. B.; Mann, M.; Meng, C. K.; Wong, S. F.; Whitehouse, C. M. *Science* **1989**, *246*, 64–71. (c) Mann, M.; Meng, C. K.; Fenn, J. B. *Anal. Chem.* **1989**, *61*, 1702–1708.

(19) Smith, R. D.; Loo, J. A.; Edmonds, C. G.; Barinaga, C. J.; Udseth, H. R. *Anal. Chem.* **1990**, *62*, 882–899.

(20) Smith, R. D.; Loo, J. A.; Barinaga, C. J.; Edmonds, C. G.; Udseth, H. R. *J. Am. Soc. Mass Spectrom.* **1990**, *1*, 53–65.

(21) (a) Fye, J. L.; Woencckhaus, J.; Jarrold, M. F. *J. Am. Chem. Soc.* **1998**, *120*, 1327–1328. (b) Chowdhury, S. K.; Katta, V.; Chait, B. T.; Williams, E. R. *Rapid Commun. Mass Spectrom.* **1990**, *4*, 81–87. (c) Rodriguez-Cruz, S. E.; Klassen, J. S.; Williams, E. R. *J. Mass Spectrom.* **1997**, *8*, 565–568. (d) Woencckhaus, J.; Hudgins, R. R.; Jarrold, M. F. *J. Am. Chem. Soc.* **1997**, *119*, 9586–9587.

(22) (a) Busch, K. L.; Glish, G. L.; McLuckey, S. A. *Mass Spectrometry/ Mass Spectrometry: Techniques and Applications of Tandem Mass Spectrometry*; VCH Publishers: New York, 1988. (b) Siuzdak, G. *Mass Spectrometry for Biotechnology*; Academic Press: San Diego, CA, 1996. (c) *Protein and Peptide Analysis by Mass Spectrometry*; Chapman, J. R., Ed.; Humana Press: Towada, NJ, 1996. (d) Yates, J. R. *Methods Enzymol.* **1996**, *271*, 351–377. (e) Gillece-Castro, B. L.; Stults, J. T. *Methods Enzymol.* **1996**, *271*, 427–448.

(23) (a) Eng, J. E.; McCormack, A. L.; Yates, J. R., III. *J. Am. Soc. Mass Spectrom.* **1994**, *5*, 976–989. (b) Yates, J. R.; Eng, J. E.; McCormack, A. L.; Schieltz, D. *Anal. Chem.* **1995**, *67*, 1426–1436. (c) Yates, J. R., III; Speicher, S.; Griffin, P. R.; Hunkapiller, T. *Anal. Biochem.* **1993**, *214*, 397–408. (d) Yates, J. R., III. *Protein. Chem.* **1997**, *16*, 495–497. (e) Yates, J. R., III; Eng, A. L.; McCormack, A. L. *Anal. Chem.* **1995**, *67*, 3202–3210.

(24) (a) Mann, M.; Wilm, M. *Anal. Chem.* **1994**, *66*, 4390–4399. (b) Clauser, K. R.; Baker, P.; Burlingame, A. L. In *Proceedings of the 44th ASMS Conference on Mass Spectrometry and Allied Topics*, Portland, OR, 1996; p 365.

(25) Hunt, D. F.; Yates, J. R., III; Shabanowitz, J.; Winston, S.; Hauer, C. R. *Proc. Natl. Acad. Sci. U.S.A.* **1986**, *83*, 6233–6237.

(26) Biemann, K. *Biomed. Environ. Mass Spectrom.* **1988**, *16*, 99–110.

(27) Biemann, K. *Methods Enzymol.* **1990**, *193*, 351–360, 455–479.

(28) Biemann, K.; Stoble, H. A. *Science* **1987**, *237*, 992–998.

(29) Roepstroff, P.; Fohlman, J. *J. Biomed. Mass Spectrom.* **1984**, *11*, 601–603.

(30) (a) Medzihradzky, K. F.; Burlingame, A. L. *Methods Enzymol.* **1994**, *6*, 284–303. (b) McCormack, A. L.; Eng, J.; Yates, J. R., III. *Methods Enzymol.* **1994**, *6*, 274–283. (c) Hunt, D. F.; Shabanowitz, J.; Yates, J. R., III. *J. Chem. Soc. Chem. Commun.* **1987**, 548–550. (d) Biemann, K.; Martin, S. A. *Mass Spectrom. Rev.* **1987**, *6*, 1–76.

(31) Papayannopoulos, I. A. *Mass Spectrom. Rev.* **1995**, *14*, 49–73.

(32) Johnson, R. S.; Martin, S. A.; Biemann, K.; Stults, J. T.; Watson, J. T. *Anal. Chem.* **1987**, *59*, 2621–2625.

(33) Wysocki, V. H. In *Proceedings of the NATO Advanced Study Institute on Mass Spectrometry in the Biological Sciences: A Tutorial*; Gross, M. L., Ed.; Kluwer Academic Publishers: Hingham, MA, 1992; pp 59–77.

(34) Alexander, A. J.; Thibault, P.; Boyd, R. K.; Curtis, J. M.; Rinehart, K. L. *Int. J. Mass Spectrom. Ion Processes* **1990**, *98*, 107–143.

(35) Ballard, K. D.; Gaskell, S. J. *Int. J. Mass Spectrom. Ion Processes* **1991**, *111*, 173–189.

(36) Wysocki, V. H.; Jones, J. L.; Dongré, A. R.; Somogyi, Á.; McCormack, A. L. In *Biological Mass Spectrometry: Present and Future*; Matsuo, T., Caprioli, R. M., Gross, M. L., Seyana, Y., Eds.; John Wiley and Sons Ltd.: New York, 1994; Chapter 2.14, pp 249–254.

(37) Jones, J. L.; Dongré, A. R.; Somogyi, Á.; Wysocki, V. H. *J. Am. Chem. Soc.* **1994**, *116*, 8368–8369.

(38) Dongré, A. R.; Jones, J. L.; Somogyi, Á.; Wysocki, V. H. *J. Am. Chem. Soc.* **1996**, *118*, 8365–8374.

(39) McCormack, A. L.; Somogyi, Á.; Dongré, A. R.; Wysocki, V. H. *Anal. Chem.* **1993**, *65*, 2859–2872.

(40) McCormack, A. L.; Jones, J. L.; Wysocki, V. H. *J. Am. Soc. Mass Spectrom.* **1992**, *3*, 859–862.

(41) Nair, H.; Somogyi, Á.; Wysocki, V. H. *J. Mass Spectrom.* **1996**, *31*, 1141–1148.

(42) Nair, H.; Wysocki, V. H. *Int. J. Mass Spectrom. Ion. Processes* **1998**, *174*, 95–100.

(43) Burlingame, A. L.; Boyd, R. K.; Gaskell, S. J. *Anal. Chem.* **1996**, *68*, 599–561 and references therein.

(44) Biemann, K. In *Mass Spectrometry*; McCloskey, J. A., Ed.; Academic Press: New York, 1990; pp 455–479.

in mass than b_n fragment ions are designated a_n ions. Immonium ions produced from various amino acids present in the peptides, as well as ions that correspond formally to the loss of H_2O and/or NH_3 from b or y fragment ions, are also represented in MS/MS spectra of protonated peptides.^{33,34,39,45–48} A general model has evolved to describe formation of the various product ions from protonated peptides. This model states that, in the absence of strongly basic residues, cleavages occur at the various amide bonds²⁷ following migration of a mobile proton^{5,38,39,49,50} to these cleavage sites(s). When a strongly basic group is present (e.g., arginine), the charge is “sequestered” at the basic site, and cleavage is initiated only if fragmentation pathways exist that do not require intramolecular proton transfer⁴⁴ or if enough energy is deposited to allow intramolecular proton transfers to occur and initiate cleavage with an appropriate rate for the instrument used. Support for this general mobile proton model comes from results of Harrison and Yalcin,⁵¹ Muller et al.,⁵² and Johnson et al.,⁵³ as well as very recently from Vaisar and Urban.⁵⁴ The concepts described as either the mobile proton model or the production of a heterogeneous population of protonated peptides (formed upon ionization and subsequent ion activation) are inherently the same.^{3,5,9,43,46,55,56} A marginal difference is that the mobile proton concept has been described in kinetic terms (i.e., some of the protonated forms may be transition states), while the heterogeneous population concept assumes the existence of different protonated forms as “real” minima on the very complicated potential energy surface. These are subtle differences, and the models are still developing and merging as a number of different groups provide data that allow refinement to produce a general model that describes peptide dissociation in the gas phase.

Although MS/MS is an important tool for peptide and protein characterization, differences exist in fragmentation efficiencies and in specific fragmentation patterns for different peptides that can hinder characterization of a peptide’s complete structure. These differences are often dictated by various structural parameters^{25,35,37–39,45,46,49,53,57,58} and include the nature of the

residues present (neutral vs acidic vs basic),^{5,37,55,59,60} the charge state of the precursor ion,^{38,40,58} the composition of the peptide backbone (amide vs N-alkylated),⁴¹ the size,^{61,62} and the conformation of the peptide.^{3,6–8,47,63,64} In the work presented here, a series of C/C*, D-, and E-containing peptides differing in the position (N- and/or C-terminal) and number (0–2) of arginine residues have been used to extend previous findings^{3,5,9,55,56} and suggestions⁶⁵ that interactions in the gas phase between acidic and basic residues affect peptide fragmentation. The peptides investigated include **RLAIFSCFR**, **RLAIFSC*FR**, **RLCIFSAFR**, **RLC*IFSAFR**, **RLCIFSCFR**, **RLC*IFSC*FR**, **RLDIFSDFR**, **RLDIFSDF**, **LDIFSDFR**, **LDIFSDF**, **RLEIFSEFR**, and **LEIFSEFR**. Previous research focusing on the activation and fragmentation of peptides has been carried out using a variety of mass spectrometric methods that utilize collisions with gaseous atoms or molecules, surfaces, or photons. These methods include low-^{25,26,66,67} and high-energy collision-induced dissociation (CID),^{20,68} surface-induced dissociation (SID),^{22,25–30,45,69–71} sustained off-resonance irradiation (SORI),^{72,73} and photodissociation, including blackbody infrared radiative dissociation (BIRD).^{72,74} Three of these methods [SID in a quadrupole tandem mass spectrometer, high-energy CID in a hybrid sector/time-of-flight (TOF) mass spectrometer, and

(45) Bean, M. F.; Carr, S. A.; Thorne, G. C.; Reilly, M. H.; Gaskell, S. *J. Anal. Chem.* **1991**, *63*, 1473–1481.

(46) Poulter, L.; Taylor, L. C. E. *Int. J. Mass Spectrom. Ion Processes* **1989**, *91*, 183–197.

(47) Ballard, K. D.; Gaskell, S. J. *J. Am. Chem. Soc.* **1992**, *114*, 64–71.

(48) (a) Hunt, D. F.; Kishnamurthy, T.; Shabanowitz, J.; Griffin, P.; Yates, J. R., III; Martino, P. A.; McCormack, A. L.; Hauer, C. R. In *Mass Spectrometry of Peptides*; Desiderio, D., Ed.; CRC Press: Boca Raton, FL, 1990; p 139. (b) Hunt, D. F.; Alexander, J. E.; McCormack, A. L.; Martino, P. A.; Michel, H.; Shabanowitz, J. In *Protein Chemistry Techniques II*; Villafranca, J. J., Ed.; Academic Press: New York, 1991; pp 455–465. (c) Hunt, D. F.; Henderson, R. A.; Shabanowitz, J.; Sakaguchi, K.; Michel, H.; Sevilir, N.; Cox, A. L.; Appella, E.; Engelhard, V. H. *Science* **1992**, *255*, 1261–1263. (d) Hunt, D. F.; Michel, H.; Dickinson, T. A.; Shabanowitz, J.; Cox, A. L.; Sakaguchi, K.; Appella, E.; Grey, H. M.; Sette, A. *Science* **1992**, *256*, 1817–1820.

(49) Dongré, A. R.; Somogyi, Á., Wysocki, V. H. *J. Mass Spectrom.* **1996**, *31*, 339–350.

(50) Nold, M. J.; Wesdemiotis, C.; Yalcin, T.; Harrison, A. G. *Int. J. Mass Spectrom. Ion Processes* **1997**, *164*, 137–153.

(51) Harrison, A. G.; Yalcin, T. *Int. J. Mass Spectrom. Ion Processes* **1997**, *165/167*, 339–347.

(52) Mueller, D. R.; Eckersley, M.; Richter, W. *Org. Mass Spectrom.* **1988**, *23*, 217–222.

(53) Johnson, R. S.; Krylov, D.; Walsh, K. A. *J. Mass Spectrom.* **1995**, *30*, 386–387.

(54) Vaisar, T.; Urban, J. *J. Mass Spectrom.* **1998**, *33*, 505–524.

(55) Cox, K. A.; Gaskell, S. J.; Morris, M.; Whiting, A. *J. Am. Soc. Mass Spectrom.* **1996**, *7*, 522–531.

(56) Summerfield, S. G.; Cox, K. A.; Gaskell, S. J. *J. Am. Soc. Mass Spectrom.* **1997**, *8*, 25–31.

(57) (a) Gaskell, S. J.; Reilly, M. H. *Rapid Commun. Mass Spectrom.* **1988**, *2*, 188–191. (b) Kenny, P. T.; Nomoto, M. K.; Orlando, R. *Rapid Commun. Mass Spectrom.* **1992**, *6*, 95–97. (c) Fabris, D.; Kelly, M.; Murphy, C.; Wu, Z.; Fenselau, C. *J. Am. Soc. Mass Spectrom.* **1993**, *4*, 652–661.

(58) Tang, X.-J.; Thibault, P.; Boyd, R. K. *Anal. Chem.* **1993**, *65*, 2824–2834.

(59) (a) Summerfield, S. G.; Gaskell, S. J. *Int. J. Mass Spectrom. Ion Processes* **1997**, *166*, 509–521. (b) Barinaga, C. J.; Edmonds, C. G.; Udseth, H. R.; Smith, R. D. *Rapid Commun. Mass Spectrom.* **1989**, *3*, 160–164.

(60) Qin, J.; Chait, B. T. *J. Am. Chem. Soc.* **1995**, *117*, 5411–5412.

(61) Downard, K. M.; Biemann, K. *Int. J. Mass Spectrom. Ion Processes* **1995**, *148*, 191–202.

(62) Jones, J. L.; Dongré, A. R.; Nair, H.; Somogyi, Á.; Wysocki, V. H. In *Proceedings of the 43rd ASMS Conference on Mass Spectrometry and Allied Topics*, Atlanta, GA, 1995; p 1333.

(63) (a) Dongré, A. R.; Hayward, M. J.; Wysocki, V. H. In *Proceedings of the 43rd ASMS Conference on Mass Spectrometry and Allied Topics*, Atlanta, GA, 1995; p 628. (b) Wu, Q.; Van Orden, S.; Cheng, X.; Bakhtiar, R.; Smith, R. D. *Anal. Chem.* **1995**, *67*, 2498–2509.

(64) Thorne, G. C.; Ballard, K. D.; Gaskell, S. J. *J. Am. Soc. Mass Spectrom.* **1990**, *1*, 249–257.

(65) Nair, H.; Wysocki, V. H.; Summerfield, S. G.; Gaskell, S. J. In *Proceedings of the 44th ASMS Conference on Mass Spectrometry and Allied Topics*, Portland, OR, 1996; p 464.

(66) (a) Tang, X.-J.; Thibault, P.; Boyd, R. K. *Anal. Chem.* **1993**, *65*, 2824–2834. (b) Tang, X.-J.; Boyd, R. K. *Rapid Commun. Mass Spectrom.* **1992**, *6*, 651–657. (c) Yost, R. A.; Boyd, R. K. In *Methods Enzymol.* **1990**, *193*, 154–200.

(67) (a) Carr, S. A.; Hemling, M. E.; Bean, M. F.; Roberts, G. D. *Anal. Chem.* **1991**, *63*, 2902–2824. (b) Gross, M. L. In *Methods Enzymol.* **1990**, *193*, 131–153. (c) Tomer, K. B. *Mass Spectrom. Rev.* **1989**, *8*, 445–482, 483–511.

(68) (a) Smith, R. D.; Barinaga, C. J.; Udseth, H. R. *J. Phys. Chem.* **1989**, *93*, 5019–5022. (b) Loo, J. A.; Edmonds, C. G.; Smith, R. D. *Science* **1990**, *248*, 201–204. (c) Loo, J. A.; Edmonds, C. G.; Smith, R. D. *Anal. Chem.* **1991**, *63*, 2488–2499.

(69) Wysocki, V. H.; Dongré, A. R. In *Large Ions: Their Vaporization, Detection and Structural Analysis*; Baer, T., Ng, Y., Powis, I., Eds.; John Wiley and Sons Ltd.: New York, 1996; Chapter 6, pp 145–165 and references therein.

(70) Wysocki, V. H.; Ding, J.; Jones, J. L.; Callahan J. H.; King, F. L. *J. Am. Soc. Mass Spectrom.* **1992**, *3*, 27–32.

(71) (a) Meot-Ner, M.; Dongré, A. R.; Somogyi, Á.; Wysocki, V. H. *Rapid Commun. Mass Spectrom.* **1995**, *9*, 829–836. (b) Hayward, M. J.; Park, F. D. S.; Phelan, L. M.; Bernasek, S. L.; Somogyi, Á.; Wysocki, V. H. *J. Am. Chem. Soc.* **1996**, *118*, 8375–8380. (c) Vékey, K.; Somogyi, Á.; Wysocki, V. H. *Rapid Commun. Mass Spectrom.* **1996**, *10*, 911–918. (d) Dongré, A. R.; Wysocki, V. H. *Org. Mass Spectrom.* **1994**, *29*, 700–702. (e) Kane, T. E.; Somogyi, Á.; Wysocki, V. H. *Org. Mass Spectrom.* **1993**, *28*, 1665–1673. (f) Callahan, J. H.; Somogyi, Á., Wysocki, V. H. *Rapid Commun. Mass Spectrom.* **1993**, *7*, 693–699.

(72) Price, W. D.; Schnier, P. D.; Williams, E. R. *Anal. Chem.* **1996**, *68*, 859–866.

(73) Senko, M. W.; Speir, J. P.; McLafferty, F. W. *Anal. Chem.* **1994**, *66*, 2801–2808.

(74) Jockusch, R. A.; Schnier, P. D.; Price, W. D.; Strittmatter, E. F.; Demirev, P. A.; Williams, E. R. *Anal. Chem.* **1997**, *69*, 1119–1126.

SORI-CID in a Fourier transform mass spectrometer (SID, keV-CID, and SORI-CID, respectively)] are utilized in the research described below because they deposit different distributions of internal energy and allow different time frames for dissociation.

Both the singly and doubly protonated peptides have been studied, and their product ion spectra are reported. Moreover, specific fragmentation product ions are observed which appear to be a consequence of specific interactions that sequester charge and allow initiation of cleavage by the acidic hydrogen of the acidic amino acid residue(s). A plausible reactive structure for these protonated peptides is proposed to account for the observed and enhanced product ions. This structure provides evidence for the predisposition of secondary structure of peptides in the gas phase. The positions of ESI/SID fragmentation efficiency curves are also obtained for most of these peptides. The relative shifts of the ESI/SID fragmentation efficiency curves within this series of peptides, where the type of acidic residue and the number of basic residues are varied, are reported and lend additional experimental evidence for the mobile proton model.

Experimental Section

Peptide Synthesis. The synthetic peptides used were prepared using multiple solid-phase synthesis protocols outlined by Atherton and Sheppard.^{75,76} 9-Fluorenylmethoxycarbonyl (Fmoc) derivatives of the various amino acids⁷⁷ required were purchased from Advanced Chemtech (Louisville, KY). The C-terminal residues required for peptide synthesis were purchased already attached to resins from Calbiochem/Novabiochem (San Diego, CA). Once each synthetic peptide was precipitated in diethyl ether, its purity and identity were checked by mass spectrometry. The following peptides were synthesized: **RLAIFSCFR**, **RLCIFSAFR**, **RLCIFSCFR**, **RLDIFSDFR**, **RLDIFSDF**, **LDIFSDF**, **LDIFSDF**, **RLEIFSEFR**, and **LEIFSEFR**.

Cysteine-to-Cysteic Acid Oxidation. Oxidation of cysteine(s) to cysteic acid(s) was performed as described by Summerfield et al.⁵⁶ The synthetic peptides containing one or two cysteine residue(s) were dried, and ~70 μg was reacted with performic acid (200 μL) for 30 min. Performic acid was made by mixing 1 mL of formic acid with 100 μL of H_2O_2 (30% w/w) at ambient temperature for 1 h.

Surface-Induced Dissociation. The instrument used for the SID experiments is a quadrupole tandem mass spectrometer specifically designed for low-energy ion-surface collisions.⁷⁰ The singly and doubly protonated peptides were formed by electrospray ionization using a modified electrospray design of Chowdhury et al.⁷⁸ and Papac et al.⁷⁹ Peptide analytes were dissolved in a 70/30% (v/v) mixture of methanol/ H_2O containing 1% acetic acid to give the appropriate concentration (~30–50 pmol/ μL)³⁸ and sprayed at atmospheric pressure from a syringe needle held at 4.2–4.7 kV (flow rate of 2 $\mu\text{L}/\text{min}$) toward a metal capillary (120 V). The temperature of the metal capillary was maintained at 120 $^\circ\text{C}$ to ensure proper desolvation of the ions. The desolvated ions were directed toward a skimmer cone (90 V), after

(75) Atherton, E.; Sheppard, R. C. In *Solid-Phase Peptide Synthesis: A Practical Approach*; Rickwood, D., Hames, B. D., Eds.; IRL Press at Oxford University Press: Oxford, UK, 1989.

(76) Deprotection was performed by using piperidine (50%) in dimethylformamide (DMF). Coupling reactions between successive L-amino acid residues were performed in a solution of DMF containing a 2–4-fold excess of *N*-hydroxybenzotriazole dihydrate (HOBt), benzotriazole-1-yl-oxy-tris(dimethylamino)-phosphonium hexafluorophosphate (BOP; Castro's reagent), diisopropylethylamine (DIEA), and the appropriate Fmoc-protected amino acid. The synthesized peptides were removed from the resin and deprotected using a mixture of 95% trifluoroacetic acid (TFA), 2.5% H_2O , and 2.5% anisole.

(77) The amino acid residues employed requiring side-chain protection are as follows: Fmoc-L-arginine, 2,2,5,7,8-pentamethylchroman-6-sulfonyl (Pmc); Fmoc-L-cysteine, *S*-trityl (Trt); Fmoc-L-serine, *tert*-butyl; Fmoc-L-glutamic acid, *tert*-butyl; Fmoc-L-aspartic acid, *tert*-butyl.

(78) Chowdhury, S. K.; Katta, V.; Chait, B. T. *Rapid Commun. Mass Spectrom.* **1990**, *4*, 81–87.

(79) Papac, D. I.; Schey, K. L.; Knapp, D. R. *Anal. Chem.* **1991**, *63*, 1658–1660.

which they entered into the high-vacuum region of the mass spectrometer, where they were analyzed and detected. The custom-built tandem mass spectrometer has been described previously.^{38,49,70} Briefly, it consists of two 4000-u Extrel quadrupoles positioned at 90 $^\circ$ with a surface positioned at the intersection of the ion optical paths of the quadrupoles. Following mass selection of the protonated peptide ion of interest by the first quadrupole, the selected ions are collided with the surface at a specific laboratory collision energy. The product ions formed by the internal excitation and subsequent dissociation of the parent ions are then analyzed by the second quadrupole.

Fragmentation efficiency curves, $\Sigma(\text{fragment ion signal intensities})/[(\text{parent ion signal intensity}) + \Sigma(\text{fragment ion signal intensities})]$ vs collision energy, were plotted by fitting a logistic curve to the data points. The SID (laboratory) collision energy was controlled by the potential difference between the ion source skimmer cone and the surface. It should be noted that, for multiply charged ions, the potential difference is multiplied by the number of charges to obtain the collision energy. SID mass spectra were obtained over a range of collision energies, and the fragmentation efficiency curves reported here represent the average of a minimum of two data sets.

The chemically modified surface used in the SID experiments was a self-assembled monolayer film of octadecanethiol or 2-(perfluorooctyl)ethanethiol on gold.⁸⁰ Gold surfaces (1000 \AA of vapor-deposited gold on silica)^{70,81,82} were obtained from Evaporated Metal Films (Ithaca, NY) and cleaned by using a UV cleaner (UV-Clean, Boekel, Philadelphia, PA) as previously described.³⁸ A 1 mM solution (in ethanol) of octadecanethiol [or 2-(perfluorooctyl)ethanethiol] was prepared and allowed to react with the clean vapor-deposited gold surfaces for a minimum of 24 h. The self-assembled monolayer surfaces were rinsed with 4–6 portions of ethanol prior to insertion into the instrument.^{38,83}

Sustained Off-Resonance Irradiation. A Bruker 7-T Fourier transform mass spectrometer (FTMS)⁸⁴ combined with an Analytica electrospray ionization source was used. The CID activation method employed was sustained off-resonance irradiation (SORI),⁸⁵ a slow multistep activation process in which ion dissociation processes that occur in the several millisecond to second time scale can be observed. The collision gas pulsed into the ion cyclotron resonance (ICR) cell was CO_2 . For the SORI-CID experiments, the radio frequency (rf) irradiation was offset by 700 Hz from the resonance frequency of the selected ions.^{73,85} The peptide solutions (5 μM) were electrosprayed (4 kV) into the vacuum system at a flow rate of 0.5 $\mu\text{L}/\text{min}$ using a Harvard Apparatus syringe pump. A glass capillary coated with metal on both ends transfers the ions from atmospheric pressure into the vacuum system. Desolvation of the sample was achieved by heating the capillary with counterflow N_2 gas at 200 $^\circ\text{C}$.

High-Energy Collision-Induced Dissociation. A JEOL HX 110A sector (E/B) instrument (JEOL, U.S.A.) was modified by the "in-line" addition of a 6-ft-long time-of-flight (TOF) tube to create the hybrid instrument used for the high-energy CID studies.⁸⁶ Samples were prepared for electrospray ionization as described above and introduced

(80) (a) Porter, M. D.; Bright, T. B.; Allara, D. L.; Chidsey, C. E. D. *J. Am. Chem. Soc.* **1987**, *109*, 3559–3568. (b) Laibinitis, P. E.; Whitesides, G. M.; Allara, D. L.; Tao, Y.-T.; Parikh, A. N.; Nuzzo, R. G. *J. Am. Chem. Soc.* **1991**, *113*, 7152–7167. (c) Bryant, M. A.; Pemberton, J. E. *J. Am. Chem. Soc.* **1991**, *113*, 8284–8293. (d) Li, Y.; Huang, J.; McIver, R. T., Jr.; Hemminger, J. C. *J. Am. Chem. Soc.* **1992**, *114*, 2428–2432. (e) Ullman, A. *Chem. Rev.* **1996**, *96*, 1533–1554.

(81) Morris, M. Riederer, D. E., Jr.; Cooks, R. G.; Ast, T.; Chidsey, C. E. D. *Int. J. Mass Spectrom. Ion Processes* **1992**, *122*, 181–217.

(82) Winger, B. E.; Julian, R. K., Jr.; Cooks, R. G.; Chidsey, C. E. D. *J. Am. Chem. Soc.* **1991**, *113*, 8967–8969.

(83) Somogyi, A.; Kane, T. E.; Ding, J.-M.; Wysocki, V. H. *J. Am. Chem. Soc.* **1993**, *115*, 5275–5283.

(84) Marshall, A. G.; Grosshans, P. B. *Anal. Chem.* **1991**, *63*, 215A–229A.

(85) Gauthier, J. W.; Trautman, T. R.; Jacobson, D. B. *Anal. Chim. Acta* **1991**, *246*, 211–225.

(86) (a) Nikolaev, E.; Somogyi, A.; Gu, C.; Brechi, L.; Finch, J. W.; Martin, C. D.; Samuelson, G. L.; Wysocki, V. H. In *Proceedings of the 46th ASMS Conference on Mass Spectrometry and Allied Topics*, Orlando, FL, 1998; pp 41. (b) Tsapralis, G.; Nair, H.; Somogyi, A.; Zhong, W.; Futrell, J. H.; Summerfield, S. G.; Gaskell, S. J. In *Proceedings of the 46th ASMS Conference on Mass Spectrometry and Allied Topics*, Orlando, FL, 1998; p 633.

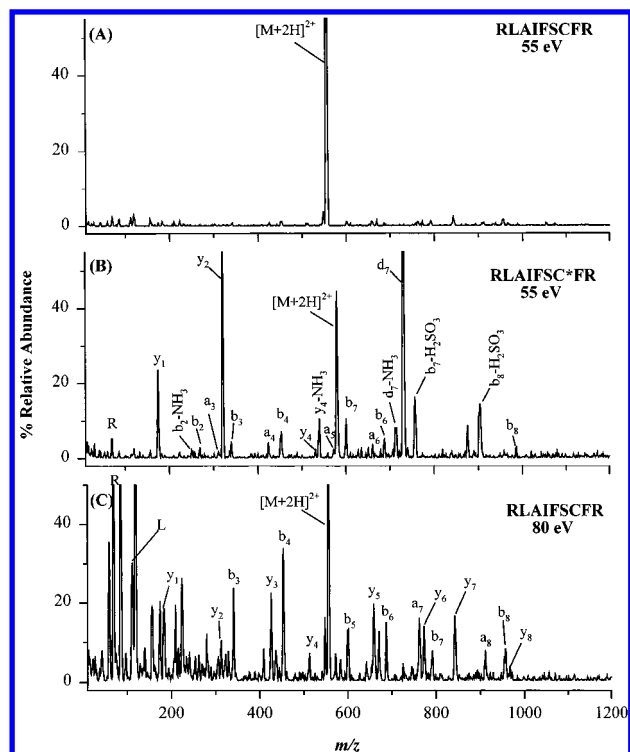


Figure 1. ESI/SID spectra of doubly protonated (A) *RLAIFSCFR* and (B) *RLAIFSC*FR* at a collision energy of 55 eV and (C) *RLAIFSCFR* at a collision energy of 80 eV on a 2-(perfluorooctyl)ethanethiolate ($\text{CF}_3(\text{CF}_2)_7\text{CH}_2\text{CH}_2\text{SAu}$) monolayer surface (C* denotes cysteic acid).

into the sector-TOF using the Analytica electrospray source. In some cases (e.g., *RLDIFSD* and *LDIFSDFR*), singly charged precursor ions were also generated by the FAB source of the sector instrument (Xe gun; glycerol:thioglycerol:*m*-nitrobenzoic acid = 2:1:1 matrix containing 1% trifluoroacetic acid). Helium was used as a collision gas at an indicated manifold pressure of $(6\text{--}10) \times 10^{-7}$ Torr. Note that the pressure was not measured directly in the CID collision chamber (which is differentially pumped) but was measured ~ 20 cm away from the chamber. In this sector-TOF instrument, the collision energy is not precisely defined. Due to an applied buncher voltage (~ 1.1 keV), the collision energy is in the range of $\sim 8.9\text{--}10.0$ keV.

Results

I. ESI/SID Product Ion Spectra and Fragmentation Efficiency Curves of Peptides Containing Cysteine and Cysteic Acid. The electrospray ionization process produced mainly doubly protonated peptides for *RLCIFSCFR*, *RLAIFSCFR*, and *RLCIFSFAFR*, while ionization of the peptides containing cysteic acid residue(s), *RLC*IFSC*FR*, *RLAIFSC*FR*, and *RLC*IFSFAFR* (cysteic acid is denoted as C*), produced both singly charged, $[M + H]^+$, and doubly charged, $[M + 2H]^{2+}$, ions. The $[M + 2H]^{2+}$ ions were then selected and collided with a fluorinated alkanethiolate surface [2-(perfluorooctyl)ethanethiolate] over a collision energy range of 20–95 eV. Figure 1A and B shows the ESI/SID spectra obtained at 55-eV collision energy for the doubly protonated peptides *RLAIFSCFR* and *RLAIFSC*FR*, respectively. For comparison, the 80-eV spectrum for the $[M + 2H]^{2+}$ peptide *RLAIFSCFR* is shown in Figure 1C. It is apparent from a comparison of the spectra presented in Figure 1A and C that the peptide incorporating a cysteine residue yields limited fragmentation at low collision energies and an extensive series of abundant sequence-specific b-, a-, and y-type ions in addition to low-*m/z* immonium product ions at collision energies > 70 eV. No selective cleavages are observed for *RLAIFSCFR* in the energy window

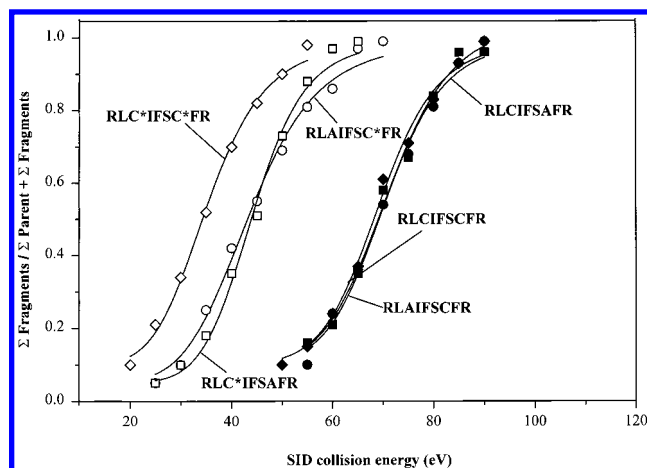


Figure 2. ESI/SID fragmentation efficiency curves of $[M + 2H]^{2+}$ ions of *RLAIFSCFR* (●), *RLCIFSFAFR* (■), *RLCIFSCFR* (◆), *RLAIFSC*FR* (○), *RLC*IFSFAFR* (□), and *RLC*IFSC*FR* (◇). The y-axis represents the ratio of $\sum(\text{fragment ion signal abundance}) / (\sum(\text{parent ion signal abundance}) + \sum(\text{fragment ion signal abundance}))$, and the x-axis represents the SID (laboratory) collision energy (eV). The ESI/SID spectra used to prepare the fragmentation efficiency curves were obtained by collision of the $[M + 2H]^{2+}$ ions with a surface prepared from 2-(perfluorooctyl)ethanethiolate ($\text{CF}_3(\text{CF}_2)_7\text{CH}_2\text{CH}_2\text{SAu}$) on vapor-deposited gold.

of 55–70 eV. In contrast, the spectrum of the C*-containing peptide (Figure 1B) is characterized by abundant d and b- H_2SO_3 product ions in addition to b- and y-type ions,^{31,35} at collision energies as low as 45 and 35 eV, for the $[M + H]^+$ and $[M + 2H]^{2+}$ ions, respectively (ESI/SID spectra not shown at these energies). It should be noted that the aggregate loss of H_2SO_3 (leading to characteristic ions such as $b_n\text{-H}_2\text{SO}_3$; Figure 1B) is further supporting evidence of the chemical modification (i.e., oxidation) in the peptides, as previously reported by Summerfield et al.⁵⁶ It is also quite apparent that the extent of fragmentation for the $[M + 2H]^{2+}$ ions of *RLAIFSCFR* (as evidenced by the relative abundance of fragment ions at 55 eV collision energy; Figure 1A) is low, whereas its C* analogue (Figure 1B) fragments efficiently at the same collision energy. In particular, cleavage C-terminal to the C* residue in the $[M + 2H]^{2+}$ ions of *RLAIFSC*FR* results in two abundant complementary fragment ions, y_2 and d_7 . A similar trend in the fragmentation patterns is observed for the other two pairs of peptides, *RLCIFSFAFR/RLC*IFSFAFR* and *RLCIFSCFR/RLC*IFSC*FR*. Enhanced cleavage C-terminal to the C* residue at position 3 in *RLC*IFSFAFR* and position 7 in *RLC*IFSC*FR* is manifested by the appearance of dominant d_3/y_6 and y_2 product ions, respectively (spectra not shown). Moreover, a strong y_5 fragment ion is also observed in the spectrum of *RLC*IFSFAFR*, which could be the result of further fragmentation of the y_6 ion and, hence, further evidence for enhanced cleavage at the C* residue. Support for sequential cleavage of y-type ions comes from the work of Ballard and Gaskell,³⁵ and the promotion of d-type ions has also been recently observed in the low-energy CID of C*-containing peptides.⁵⁶

The ESI/SID fragmentation efficiency curves obtained for the $[M + 2H]^{2+}$ C/C*-containing peptides are shown in Figure 2. A comparison of these curves shows that the peptides with either one or two cysteine residues require higher collision energies for efficient fragmentation, while their analogues containing a single C* residue require lower energies for the same extent of fragmentation. Moreover, the fragmentation efficiency curve for the peptide containing two C* residues is shifted to even lower energies compared to those of the peptides

Table 1. SID Collision Energy Corresponding to ~50% Fragmentation for Doubly Protonated Peptides Containing Acidic and Basic Residues

[peptide + 2H] ²⁺	SID energy _{50%} fragmentation (eV)
<u>RLC</u> <u>IFSC</u> <u>FR</u>	68.5
<u>RLC</u> * <u>IFSA</u> <u>FR</u>	43.6
<u>RLA</u> <u>IFSC</u> * <u>FR</u>	44.2
<u>RLC</u> * <u>IFSC</u> * <u>FR</u>	35.4
<u>RLD</u> <u>IFSD</u> <u>FR</u>	55.9
<u>RLE</u> <u>IFSE</u> <u>FR</u>	68.2

containing a single C* residue. The energy required for ~50% fragmentation (Table 1) increases for the various [M + 2H]²⁺ peptides investigated in the order of RLC*IFSC*FR < RLC*IFSAFR ≈ RLAIFSC*FR < RLCIFSCFR ≈ RLAIFSCFR ≈ RLCIFSAFR. Clearly, introduction of C* residue(s) significantly lowers the energy requirement for fragmentation in the above peptides. This is in agreement with previous observations based on low-energy CID spectra, that the fragmentation efficiency of RLCIFSCFR is low even at 60-eV laboratory collision energy,⁶⁶ while the C*-containing analogue requires only 20–30 eV for efficient but selective fragmentation.^{5,55}

II. Product Ion Spectra and Fragmentation Efficiency Curves of Peptides Containing Aspartic and Glutamic Acid. (A) Two Arginines, Two Aspartic Acids, and Two Protons: Selective Cleavages.

Figure 3A and B shows the product ion spectra of [M + 2H]²⁺ ions of RLDIFSDFR obtained by ESI/SID (55 eV) and SORI-CID (13 eV), respectively. The striking similarity between the two spectra is attributed to enhanced formation of b₇ and y₂ fragment ions caused by cleavage of the DF bond in RLDIFSDFR. In fact, at the various collision energies investigated by ESI/SID (35–85 eV), the product ion spectra of RLDIFSDFR are consistently dominated by this pair of fragment ions. Moreover, SORI-CID, a technique which favors the lowest energy dissociation pathways in peptide precursor ions,^{73,87} also results in the same b/y complementary fragment ions. Previous work performed by Summerfield et al.⁵ has also shown this cleavage to be prominent by low-energy CID, although a more complete series of b- and y-type ions indicative of greater fragmentation is also observed. Facile cleavage of peptide bonds adjacent to a D residue has been reported by SORI-CID in a FTMS.⁸⁸ Qin and Chait⁶⁰ have observed preferential cleavage of the peptide bond adjacent to D residues using a MALDI ion trap mass spectrometer, while Price et al.¹¹ have measured the Arrhenius parameters for the y₂₄⁴⁺/b₅₂⁷⁺ fragment pair of ubiquitin, which is also the result of facile cleavage at a D residue. Postsource decay (PSD) experiments on [M + H]⁺ peptide ions in a MALDI-TOF mass spectrometer⁸⁹ have provided further evidence for facile cleavage at D residues. In these experiments, the requirement of a free carboxyl group on D for such a facile cleavage was also unequivocally demonstrated by esterification studies.⁸⁹ Low-mass fragments arising from cleavage at D were not observed in the reflectron mass spectra of esterified DPRAEL, presumably because esterification blocks the carboxyl group of the D

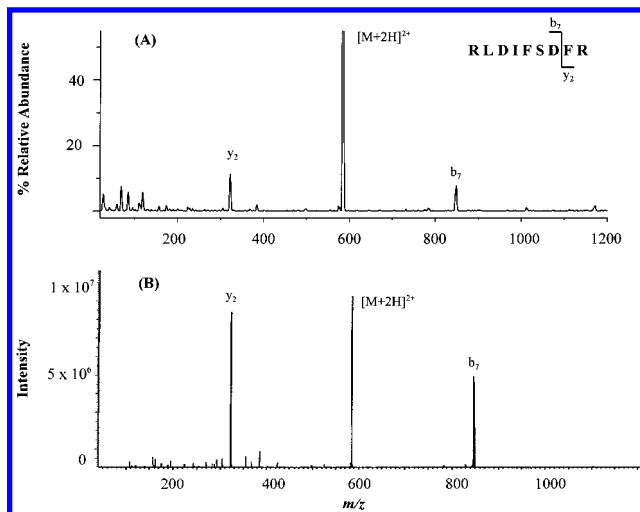


Figure 3. (A) ESI/SID spectrum of doubly protonated RLDIFSDFR at a collision energy of 55 eV on a 2-(perfluorooctyl)ethanethiolate (CF₃(CF₂)₇CH₂CH₂SAu) monolayer surface. (B) Sustained off-resonance irradiation mass spectrum in a Fourier tandem mass spectrometer of doubly protonated RLDIFSDFR at an excitation energy of 13 eV; electrospray ionization.

residue.⁸⁹ Finally, facile formation of y₁ fragment ions in DX-type dipeptides has also been observed by Harrison and Tu using low-energy CID and metastable ion studies.⁹⁰

(B) One Arginine, Two Aspartic Acids, and One Proton: Selective Cleavages. The MS/MS spectra of the [M + H]⁺ ions of RLDIFSDFR obtained by ESI/SID, SORI-CID, and high-energy CID are shown in Figure 4A, B, and C, respectively. Product ions due to cleavages at the third and seventh D residues (b₃ and b₇) are observed in all three spectra. N-Terminal product ions resulting from the loss of NH₃ (b₃ - NH₃) and C-terminal rearrangement product ions (b₇ + H₂O) are also quite strong in the ESI/SID spectrum. In addition, the SORI-CID MS/MS spectrum (Figure 4B) also shows minor b-type product ions resulting from cleavages along the peptide backbone, while abundant immonium ions and side-chain cleavage ions are generated by high-energy CID (Figure 4C). The characteristic b₃, b₃ - NH₃, b₇, and b₇ + H₂O fragment ions seen by ESI/SID are also present in relatively high abundance in the keV-CID spectrum, and these are the only strong b ions detected (other "sequence ions are a_n and not b_n ions). This observation is in sharp contrast to the findings by van Dongen et al.⁹¹ of a statistical analysis of MS/MS data obtained from [M + H]⁺ peptide ions under high-energy CID conditions. In that study, peptides containing an R residue at or near the N-terminus were found to have MS/MS spectra that were dominated by d- and a-type fragment ions with no b ions present. Our findings reinforce the view that the b₃ and b₇ fragment ions of the singly protonated RLDIFSDFR by high-energy CID parallel the enhanced cleavages adjacent to the third and seventh D residues in ESI/SID and SORI-CID. b + H₂O ions have been previously reported for a variety of peptides, including bradykinin (RP-PGFSPFR)⁶⁴ and leucine enkephalin (YGGFL).⁴⁷ A fragmentation mechanism based on ¹⁸O-labeling experiments has been proposed in which the C-terminal amino acid residue is lost concomitant with retention of one of the carboxyl oxygens at the C-terminus of the shortened peptide. Similar fragmentation has been demonstrated for metal-cationized peptides⁷⁸ as well as for synthetic peptides containing a N-terminal R residue.⁴ It is of interest that the b₇ + H₂O fragment ion of RLDIFSDFR is not observed by SORI-CID but is observed by high-energy CID.

(87) Marzluff, E. M.; Campbell, S.; Rodgers, M. T.; Beauchamp, J. L. *J. Am. Chem. Soc.* **1994**, *116*, 7787–7796.

(88) Bakhtiar, R.; Wu, Q.; Hofstadler, S. A.; Smith, R. D. *Biol. Mass Spectrom.* **1994**, *65*, 707–710.

(89) Yu, W.; Vath, J. E.; Huberty, M. C.; Martin, S. A. *Anal. Chem.* **1993**, *65*, 3015–3023.

(90) Harrison, A.; Tu, Y.-P. *J. Mass Spectrom.* **1998**, *33*, 532–542.

(91) van Dongen, W. D.; Ruijters, H. F. M.; Luinge, H.-J.; Heerma, W.; Haverkamp, J. *J. Mass Spectrom.* **1996**, *31*, 1156–1162.

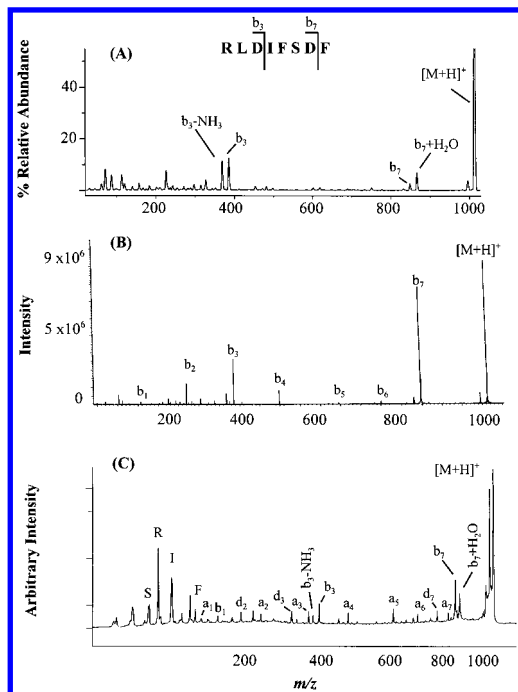


Figure 4. (A) ESI/SID spectrum of singly protonated RLDIFSDF at a collision energy of 50 eV on a 2-(perfluorooctyl)ethanethiolate ($\text{CF}_3(\text{CF}_2)_7\text{CH}_2\text{CH}_2\text{SAu}$) monolayer surface. (B) Sustained off-resonance irradiation mass spectrum in a Fourier tandem mass spectrometer of singly protonated RLDIFSDF at an excitation energy of 18.7 eV; electrospray ionization. (C) High-energy collision-induced dissociation spectrum in a linear sector time-of-flight mass spectrometer of singly protonated RLDIFSDF; collision gas is He at a pressure of 6.4×10^{-6} Torr; fast atom bombardment ionization.

The ESI/SID, SORI-CID, and keV-CID MS/MS spectra of the $[\text{M} + \text{H}]^+$ ions of LDIFSDFR are shown in Figure 5A, B, and C, respectively. Dominant y_2 and y_6 ions arising from cleavage at the second and sixth D residues are observed using all three activation methods. This is in agreement with preferential cleavage of protonated peptides adjacent to D residues, reported earlier.^{11,60,88,89}

(C) No Arginine, Two Aspartic Acids, and One Proton: Nonselective Cleavages. The ESI/SID spectrum of the $[\text{M} + \text{H}]^+$ ions of the peptide devoid of basic residues (LDIFSDF) is shown in Figure 6. Although the peptide contains acidic residues, no enhanced fragment ions are detected. Instead, N-terminal and C-terminal fragments (b_2 – b_7 and y_1 – y_5) are observed. Nonselective cleavage of the peptide backbone of LDIFSDF is also seen by SORI-CID and high-energy CID (spectra not shown). This is consistent with a heterogeneous charge distribution leading to nonselective cleavage along the peptide backbone. Moreover, it should be noted that the energy requirement for fragmentation of singly protonated LDIFSDF by SID is lower than that for the singly protonated R-containing series of peptides (LDIFSDFR and RLDIFSDF). This is consistent with previous findings on the energetics by ESI/SID of peptides with no basic residues.^{37,38}

(D) One Arginine, Two Acidic Residues, and Two Protons: Nonselective Cleavages and Energetics of Fragmentation. The influence of adding a second proton to RLDIFSDF and LDIFSDFR to generate doubly charged ions was also investigated. The SID, SORI-CID, and high-energy CID MS/MS spectra of $[\text{M} + 2\text{H}]^{2+}$ ions of RLDIFSDF and LDIFSDFR produced by ESI clearly reveal that the addition of a second proton has a dramatic effect on the fragmentation patterns of these peptides (spectra not shown). Nonselective cleavages

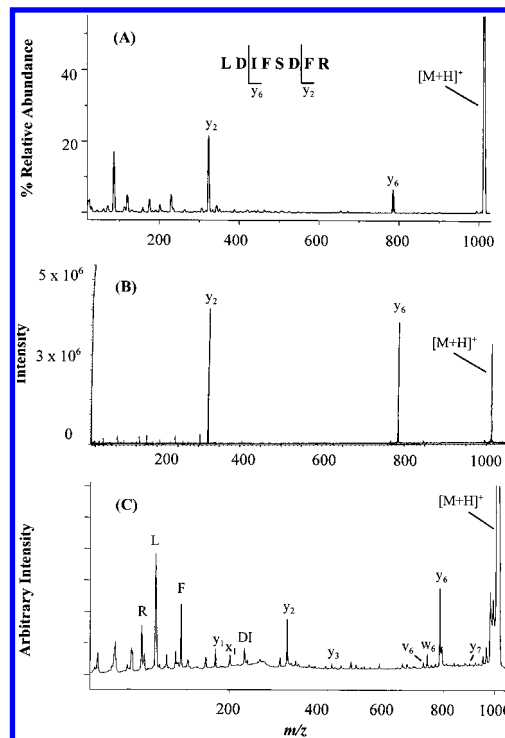


Figure 5. (A) ESI/SID spectrum of singly protonated LDIFSDFR at a collision energy of 48 eV on a 2-(perfluorooctyl)ethanethiolate ($\text{CF}_3(\text{CF}_2)_7\text{CH}_2\text{CH}_2\text{SAu}$) monolayer surface. (B) Sustained off-resonance irradiation mass spectrum in a Fourier tandem mass spectrometer of singly protonated LDIFSDFR at an excitation energy of 18.7 eV; electrospray ionization. (C) High-energy collision-induced dissociation spectrum in a linear sector time-of-flight mass spectrometer of singly protonated LDIFSDFR; collision gas is He at a pressure of 5.2×10^{-7} Torr; fast atom bombardment ionization.

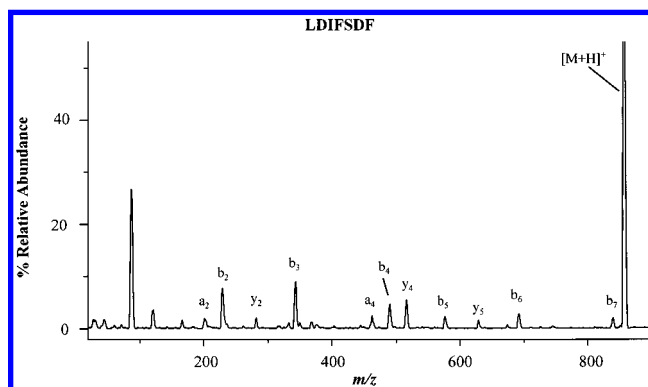


Figure 6. ESI/SID spectrum of singly protonated LDIFSDF at a collision energy of 35 eV on an octadecanethiolate ($\text{CH}_3(\text{CH}_2)_{17}\text{SAu}$) monolayer surface.

leading to MS/MS spectra that are rich in “full” sequence ions are now observed for the $[\text{M} + 2\text{H}]^{2+}$ ions, in sharp contrast to their $[\text{M} + \text{H}]^+$ ions (Figures 3 and 4). Qualitatively similar fragmentation patterns for the $[\text{M} + 2\text{H}]^{2+}$ ions of these peptides have also been observed by Summefield et al.⁵

(E) Cleavage at Glutamic Acids in RLEIFSEFR and LEIFSEFR: Kinetic Control of Diagnostic Cleavages. A series of peptides were synthesized that contain glutamic acid residues (E) in lieu of aspartic acid (D) residues, and their fragmentation spectra were obtained by ESI/SID and SORI-CID. Figure 7 shows the ESI/SID fragmentation efficiency curves of the $[\text{M} + 2\text{H}]^{2+}$ ion species of RLDIFSDF and LDIFSDFR as well as the peptides incorporating two R residues (RLDIFSDFR and RLEIFSEFR). A significant increase in the

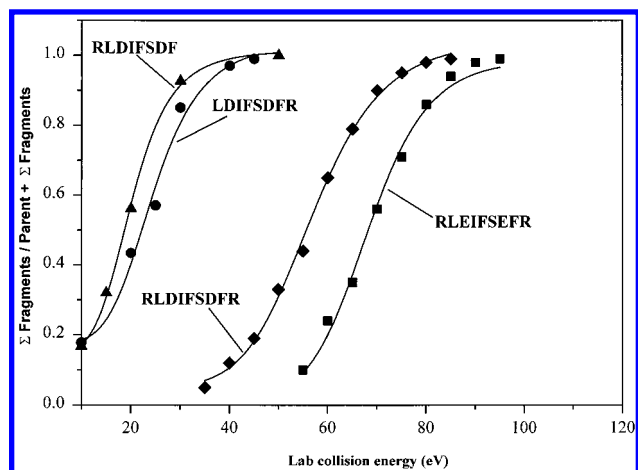


Figure 7. ESI/SID fragmentation efficiency curves of $[M + 2H]^{2+}$ ions of **RLEIFSEFR** (■), **RLDIFSDFR** (◆), **RLDIFSDF** (▲), and **LDIFSDFR** (●). The y-axis represents the ratio of $\sum(\text{fragment ion signal abundance})/\sum(\text{parent ion signal abundance}) + \sum(\text{fragment ion signal abundance})$, and the x-axis represents the SID (laboratory) collision energy (eV). The ESI/SID spectra used to prepare the fragmentation efficiency curves were obtained by collision of the $[M + 2H]^{2+}$ ions with a surface prepared from 2-(perfluorooctyl)ethanethiolate ($\text{CF}_3(\text{CF}_2)_7\text{CH}_2\text{CH}_2\text{SAu}$) on vapor-deposited gold.

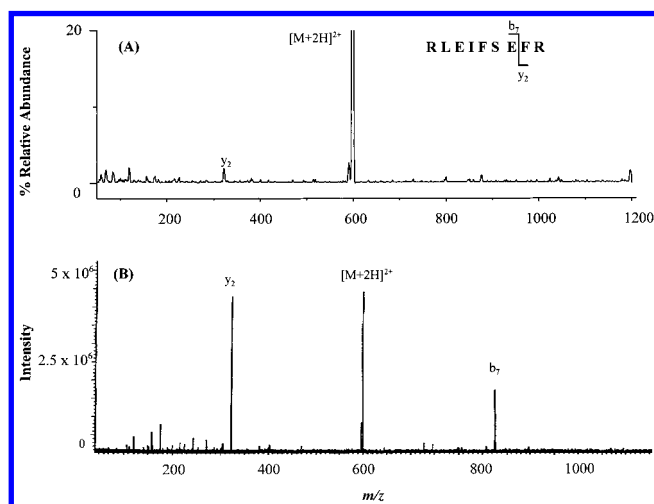


Figure 8. (A) ESI/SID at a collision energy of 55 eV on a 2-(perfluorooctyl)ethanethiolate ($\text{CF}_3(\text{CF}_2)_7\text{CH}_2\text{CH}_2\text{SAu}$) monolayer surface and (B) sustained off-resonance irradiation mass spectrum in a Fourier tandem mass spectrometer at an excitation energy of 22 eV of doubly protonated **RLEIFSEFR** (Electrospray ionization). Note that the relative abundance of the y_2 fragment ion is $<5\%$ by ESI/SID.

fragmentation efficiency (curves shifted to lower SID energies) is observed for peptides containing a single R but *two* protons. Moreover, the fragmentation efficiency of **RLEIFSEFR** is significantly decreased (shifted to higher SID energies) relative to the peptide containing two D and two R residues (**RLDIFSDFR**). This is also clearly evident from an examination of the energy required for $\sim 50\%$ fragmentation between **RLDIFSDFR** and **RLEIFSEFR** (Table 1).

The MS/MS spectral data for the $[M + 2H]^{2+}$ ions of **RLEIFSEFR** following SID and SORI-CID are shown in Figure 8A and B, respectively. In contrast to the ESI/SID and SORI-CID MS/MS spectra of $[M + 2H]^{2+}$ **RLDIFSDFR** (Figure 3), the spectra of **RLEIFSEFR** are different between the two ion-activation techniques. A preferred cleavage adjacent to the E_7 residue resulting in the b_7/y_2 fragment ion pair is dominant only by SORI-CID. y_2 fragment ions are detected

in the ESI/SID spectrum, but with very low abundance. In contrast, a relatively strong y_2 fragment ion has been observed for this doubly protonated peptide using low-energy CID in a quadrupole mass spectrometer, although other minor fragments were also observed.⁵ Preferential fragmentation adjacent to both D and E residues has been observed in peptides using a MALDI quadrupole ion trap instrument.⁶⁰ Moreover, it was noted that cleavages adjacent to E residues are observed in the ion trap as a result of the prolonged time window of the experiment (10^{-4} to >1 s), although the dissociation process(es) leading to the enhanced fragmentation at the acidic residues was not speculated upon. This is in agreement with our observations of cleavages at E seen by SORI-CID (millisecond to second time frame) but not by ESI/SID (microsecond time frame). Therefore, this cleavage (as depicted in the model shown below) can be sampled conveniently over the time frame of the SORI-CID experiments.

When R is removed from the N-terminus in **RLEIFSEFR** to generate **LEIFSEFR** and the $[M + H]^+$ ions are dissociated, y_2 and y_6 product ions result (SORI-CID spectra not shown), which are formed from cleavages at the two E residues analogous to the ones seen at the two D residues (**LDIFSDFR**; Figure 5B). The SORI-CID MS/MS results for the $[M + 2H]^{2+}$ ions of **LEIFSEFR** (spectrum not shown) also demonstrate nonselective cleavages similar to those reported previously for this peptide.⁵⁹ This again is similar to the D-containing peptide (**LDIFSDFR**, section D above) and is consistent with the second proton being highly mobile (see discussion below).

Discussion

I. Number of Charges Relative to Number of Arginine Residues as Predictor of Nonselective Fragmentation. The results presented above illustrate that the number of ionizing protons relative to the number of basic residues present in C^* -, D-, or E-containing peptides has a strong influence on the dissociation patterns of protonated peptides. Specific cleavages adjacent to acidic residues are observed when the number of ionizing protons equals the number of arginine residues in these peptides (e.g., see Figures 1B and 3–5). In contrast, nonselective cleavages yielding extensive fragmentation are seen when the number of ionizing protons is greater than the number of basic residues (e.g., for **LDIFSDFR** + $1H^+$) as shown in Figure 6, and for **RLDIFSDFR** + $2H^+$ and **LDIFSDFR** + $2H^+$). These results are consistent with the “mobile” proton model for peptide fragmentation, which describes how the population of different protonated forms of a peptide depends on the internal energy content of the peptide and the relative gas-phase basicities of the different protonation sites of the peptide. Moreover, addition of energy (e.g., by activation in MS/MS) alters this population of protonated forms (mobilizes the proton) and increases the population of protonated forms with energies higher than that of the most stable structure. Cleavage is initiated only if fragmentation pathways exist that do not require intramolecular proton transfer or if enough energy is deposited to allow intramolecular proton transfers to occur and initiate cleavage. The energy required for intramolecular proton transfer or “mobilization” depends on the amino acid composition, with energy requirements for R-containing peptides $>$ K-containing peptides $>$ nonbasic peptides. The higher energy forms produced by ion activation (e.g., collisions with gases or a surface) involve protonation or H^+ -bridging at various less basic sites. Some of these forms can fragment more easily (faster) than others, and these forms can dominate the fragmentation even when they are not dominant in the ion population, because fragmentation

in MS/MS is a kinetic process. Those forms in which the amide nitrogen is involved in protonation or H⁺-bridging, for example, fragment readily to produce sequence ions; *ab initio* and MNDO bond order calculations have previously established that the involvement of the amide nitrogen in protonation weakens the peptide bond.^{39,92} Harrison and Yalcin⁵¹ have recently prepared deuterated [M + D]⁺ ions for a variety of amino acids and peptides by chemical ionization and have shown that the added D⁺ can scramble with all labile hydrogens, including carboxylic, hydroxylic, and amidic hydrogens as well as the amino hydrogen. These results indicate that the added proton is mobile and can transfer to various sites prior to fragmentation.

These general ideas can explain the nonselective fragmentation observed in the [M + H]⁺ ions of LDIFSDF and in the [M + 2H]²⁺ ions of RLDIFSDF and LDIFSDFR. In accordance with the first ionizing proton being sequestered by the R residues in RLDIFSDF and LDIFSDFR, their nonselective fragmentation patterns can be rationalized by mobilization of the second (or excess) ionizing proton along the backbone. From this, it follows that the heterogeneous population of protonated forms produced for the peptides with one arginine, but two protons, is now responsible for the SID energy shifts between the peptides containing one vs two arginines (Figure 7). In the peptides with two arginines (RLDIFSDFR and RLEIFSEFR), the two ionizing protons are sequestered by the two R residues, making charge delocalization and nonselective fragmentation inefficient. This effect, by two ionizing protons, on the fragmentation efficiency of peptides has also been observed for [M + 2H]²⁺ ions derived from tryptic peptides when compared with their [M + H]⁺ analogues.^{19,66,93} A similar trend for the [M + H]⁺ and [M + 2H]²⁺ ions of *des*-Arg⁹ bradykinin (RPPGFSPF) and *des*-Arg¹ bradykinin (PPGFSPFR) has also been reported.³⁸ Moreover, the fragmentation efficiencies for different protonation states (3+ to 6+) of mellitin have been determined, and the data clearly reveal an increase in fragmentation efficiency with increasing charge state.⁵⁹ The latter observation has been explained in terms of increased protonation of the peptide backbone (mobile protons). What is novel about the results presented here is that these peptides contain acidic residues in addition to the basic arginines. The ions with two arginines and two acidic residues fragment more readily than peptides with two arginines and one acidic residue, which fragment more readily than peptides with no acidic residues (see Table 1). Furthermore, peptides with acidic residues in addition to arginine fragment *selectively*, with enhanced cleavage adjacent to specific acidic residues.

It has been proposed in the literature that the acidic and basic side chains present in a peptide chain might interact, forming a neutral bridge or zwitterion structure, and thus allow formation of a heterogeneous population of protonated forms of the peptide because the arginine involved in the salt bridge is not available for protonation and the added proton can locate at any of a variety of different positions along the chain (e.g., at carbonyl oxygens along the backbone). An alternative explanation is that protonation does occur at arginine, even in the presence of acidic residues. Because the arginine side chain is a strong base and protonated arginine is therefore a weak acid, the acidic hydrogen(s) of the carboxylic acid group(s) can serve as the "active" proton(s) that initiate low-energy cleavages. These possibilities are evaluated below, based on the data presented in the Results.

II. The Role of Acid–Base Interactions in Protonated Peptides on Selective Cleavages. It is clear from the above experimental observations that the incorporation of acidic residues leads to significant differences in fragmentation patterns of peptides. The question of whether the observed differences in the fragmentation of peptides with and without acidic residues are caused by intramolecular acid–base interactions as suggested previously,^{3,55} or simply related to some independent property of the acidic residues, is addressed below. Figure 9 shows three different orientations (A, B, and C) of acidic side chain(s) relative to the basic residue(s) for [M + H]⁺ peptide ions. Figure 9A depicts an interaction between the acidic proton of the acidic residue and the amide nitrogen of the residue C-terminal to it, while Figure 9B and C depicts two types of possible acid–base interactions. A neutral bridge is shown in Figure 9B, and solvation of the charge on protonated arginine by the side chain of an acidic residue (C*, D, and E) is shown in Figure 9C. It should be noted that the interaction between the amide nitrogen and the acidic hydrogen shown in Figure 9A may also be possible when protonated arginine is solvated by the various carboxylate/sulfonate groups (Figure 9C). If the interactions of 9C and 9A result at the same acidic side chain, the result is a salt bridge. While any of these three interactions is plausible, they need to be evaluated in light of the mass spectral data obtained, and in terms of possible fragmentation mechanisms such as those outlined by Yu et al.⁸⁹

(A) No Acid–Base Interaction. The simplest scenario (Figure 9A) is one in which the side chain of the acidic residue interacts with the amide nitrogen of the bond C-terminal to it and does not interact with the side chain of the basic residue. The presence of an aspartic residue in the peptide backbone has been shown by MALDI-TOF and MALDI ion trap mass spectrometry to result in facile cleavage of the amide bond C-terminal to this residue.⁸⁸ To account for this facile cleavage, Yu et al.⁸⁹ have proposed a mechanism wherein the acidic hydrogen is transferred to the adjacent (C-terminal) amide nitrogen, resulting in enhanced cleavage of that specific amide bond. A model for the peptides studied in our work, based on this mechanism, is presented in Scheme 1. Such a model can be used to explain the enhanced cleavage of the doubly protonated RLAIFSC*FR at the C* residue (i.e., the prominent d₇ and y₂ fragment ions; Figure 1B, Scheme 1A) and the seventh D residue in the RLDIFSDFR peptide (i.e., the prominent b₇ and y₂ fragment ions; Figure 3, Scheme 1B). In principle, this mechanism can also be used to rationalize the shift in the ESI/SID fragmentation efficiency curves between doubly protonated RLAIFSC*FR and RLDIFSDFR on the basis of the differences in the relative acidities of the two residues C* and D (C* is more acidic). Furthermore, it can also be argued that the relatively low fragmentation efficiency (Figure 7) of the doubly protonated RLEIFSEFR compared to those of RLDIFSDFR and RLAIFSC*FR is attributed to the additional –CH₂ group in E, which could slow the formation of a stable intermediate necessary for the cleavage.

While the mechanism of Yu et al.⁸⁹ is attractive, the combined MS/MS spectral data presented above dictate that it should be extended in order to explain the predominant fragmentation processes occurring in the peptides investigated. It is clearly evident from the spectra of doubly protonated RLDIFSDFR that cleavage of the amide bond adjacent to D at the seventh position is favored over cleavage at the D residue at the third position (Figure 3). This observation cannot be explained exclusively on the basis of the model shown in Figure 9A and the

(92) Somogyi, Á.; Wysocki, V. H.; Mayer, I. *J. Am. Chem. Soc.* **1994**, 116, 704–717.

(93) Covey, T. R.; Huang, B. C.; Henion, J. D. *Anal. Chem.* **1991**, 63, 1193–1200.

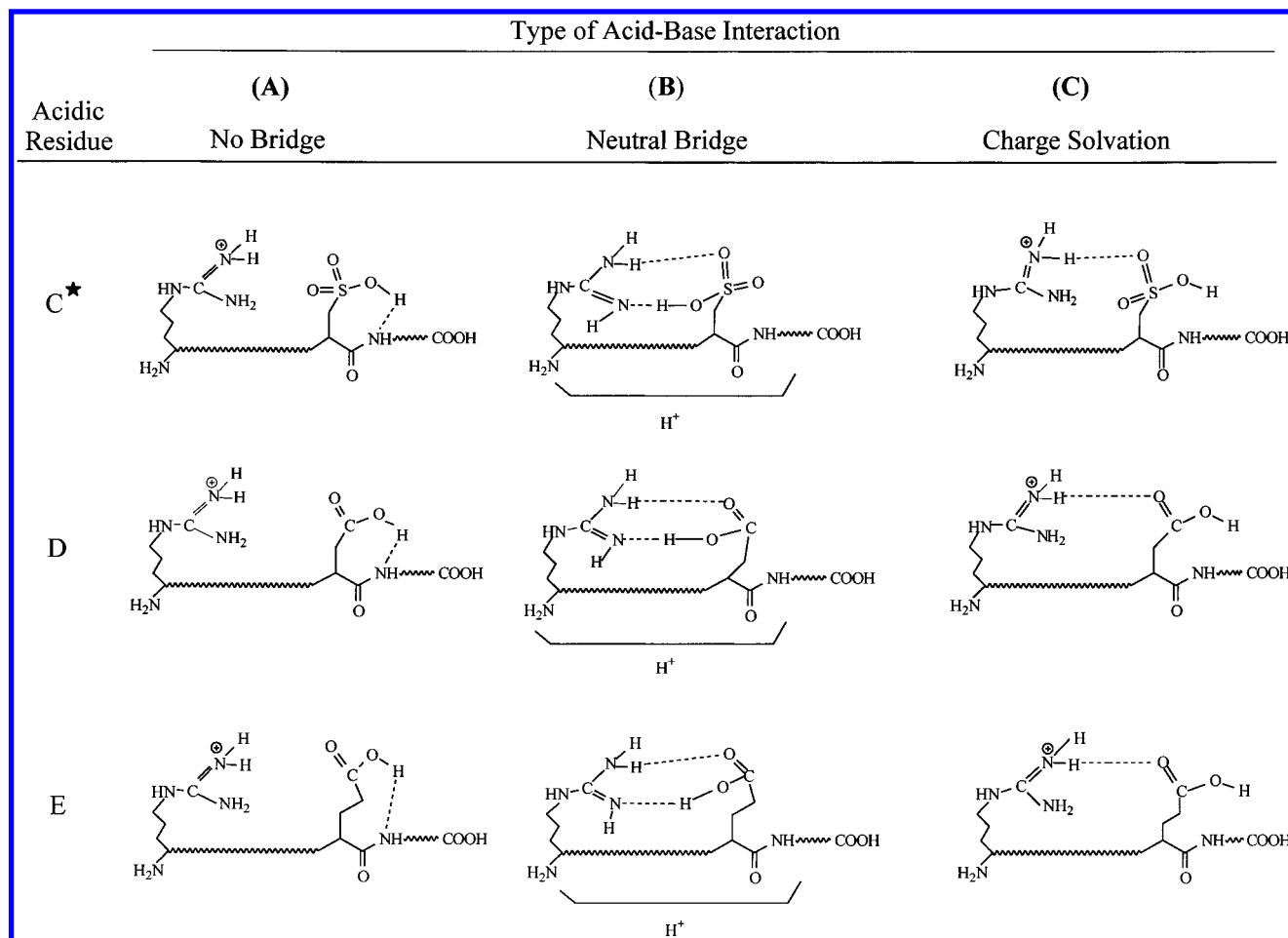


Figure 9. Plausible orientations of the N-terminal basic (R) residue and the acidic residue (C*, D, and E) showing (A) no acid–base interactions, (B) acid–base interaction via a neutral bridge resulting in charge heterogeneity, and (C) acid–base interaction via charge solvation where the added (ionization) proton is involved in the bridging.

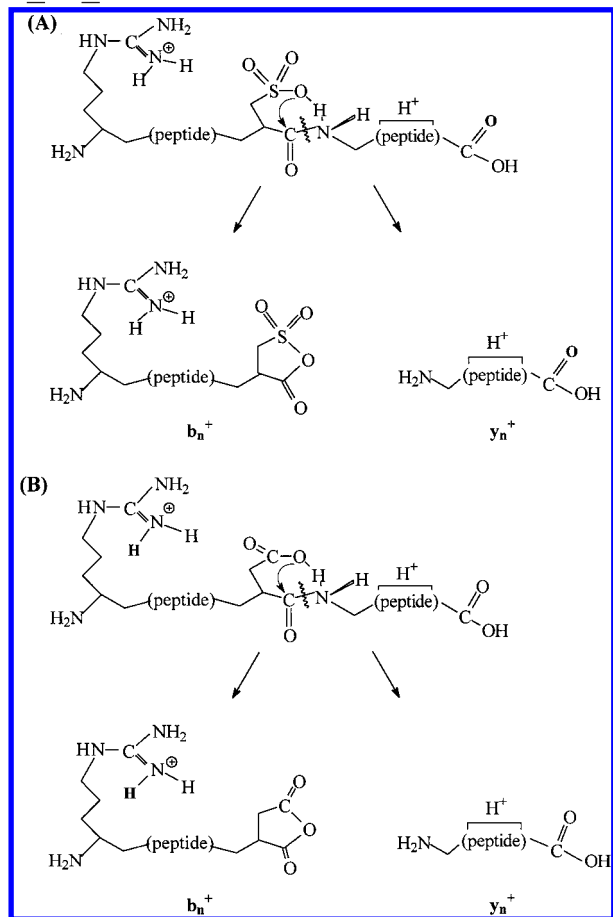
mechanism in Scheme 1A. The SID spectra of peptides containing C* presented here are, in general, qualitatively similar to the low-energy CID spectra reported previously.^{5,55} Moreover, the formation of d and b-H₂SO₃ ions in the low-energy CID spectra of doubly protonated *RLAIFSC*FR* and *RLC*IFSAFR* has been studied more recently in detail using MS/MS/MS and deuterium labeling.⁵⁶ Based on these results, Summerfield et al.⁵⁶ proposed that the formation of these ions may be triggered by an acid–base interaction between C* and the basic guanidino group of R. In turn, the two additional types of acid–base interactions, shown in Figure 9B and C, are now considered in order to explain the specificity in cleavage location observed by ESI/SID, SORI–CID, and high-energy CID in the peptides that contain both acidic and basic residues.

(B) Acid–Base Interaction via a Neutral Bridge. Figure 9B shows an interaction via a neutral bridge between the acidic side chain of C*, D, or E, and the guanidino group of an R side chain. Such an interaction might prevent protonation at that R residue side chain leading to charge-site heterogeneity. According to this model, in a population of doubly protonated precursors with oxidized cysteine (*RLC*IFSAFR* and *RLAIFSC*FR*), one proton may be located at an R side chain and the other at a multitude of possible sites along the peptide backbone, while the other R side chain is bridged to the C* side chain. The proton that is heterogeneous with respect to its location in a population of protonated peptides can, with equal probability, enhance charge-directed cleavage along the peptide backbone at any one given amide bond. The presence of such

a heterogeneous population of protonated forms of the peptide can, indeed, enhance the fragmentation efficiency, as observed in Figure 2. However, it would be expected that the spectra arising from such a heterogeneous population of [M + 2H]²⁺ ions would contain a nonselective distribution of fragment ions such as those seen for the cysteine-containing peptide in Figure 1C. The specific sites of favored fragmentation (at the amide bond of the seventh residue) observed for [M + 2H]²⁺ of *RLAIFSC*FR*, *RLDIFSDFR* by ESI/SID and SORI–CID, as well as for *RLEIFSEFR* by SORI–CID, suggest that these fragmentation patterns cannot be explained on the basis of an interaction via the neutral bridge between the acidic and basic residues and the R residue.

(C) Charge Solvation. Specificity in the location of cleavage indicates that the location of the proton inducing the cleavage is an important factor in determining the predominant fragment ions in a spectrum. We now turn to the charge solvation model shown in Figure 9C for possible insight into the role of the proton in the fragmentation of the peptides. Figure 9C shows the arginine-sequestered ionizing proton being solvated by the side chain of the acidic and basic residues. In principle, such a solvation can cause or prevent specific cleavage at the acidic residue due to lack of mobility of the added proton. Moreover, charge solvation can occur between any of the two R residues and the carboxylate moieties on the acidic residues or the C-terminus. Based on previous low-energy CID investigations,⁵ it has been suggested that, in doubly protonated *RLAIFSC*FR*, the protonated N-terminal R interacts with the acidic side chain

Scheme 1. Formation of b_7 and y_2 Pair (A) upon Fragmentation of the Doubly Protonated **RLAIFSC*FR** Based on the Mechanism Proposed by Yu et al.^{50a} and (B) by a Similar Mechanism in the Doubly Protonated Peptide **RLDIFSDFR**

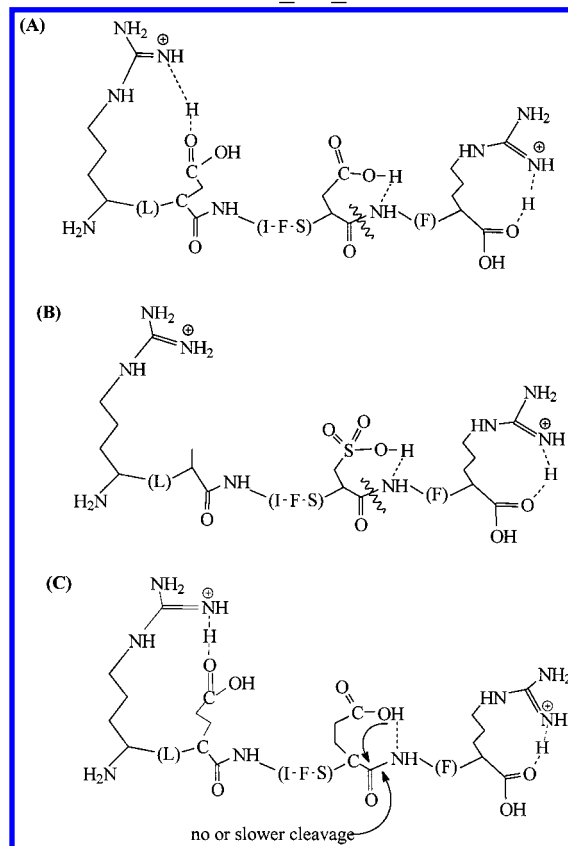


^a Subsequent loss of H_2SO_3 and CO can lead to the observed d_7 fragment ion shown in Figure 1B.

of the C^* residue. Based on such an interaction, a mechanism for the formation of d_7 ions, in which the neutral N-terminal R side chain H-bonds to the C^* residue at the seventh position, has been proposed. Moreover, a similar mechanism was also proposed for the formation of the b_7/y_2 fragment ion pair in doubly protonated **RLDIFSDFR**.⁵ Such an interaction was hypothesized to prevent sequestration of the proton by the R residue side chain, an event which subsequently mobilizes the proton and facilitates its transfer along the peptide backbone. This should result in improved fragmentation of the amide bonds and can, in principle, explain the overall improved fragmentation efficiency of the **RLDIFSDFR** peptide. Based on the present data, however, the specific enhanced cleavage at the D residue in position 7 and the lack thereof at the third residue (D) cannot be explained by this hypothesis. Moreover, such a hypothesis cannot explain the preferred cleavages detected at all D and E residues in $[\text{M} + \text{H}]^+$ ions of fibrinopeptide A (**ADSGEGD-FLAEGGGVR**) by ESI/SID and SORI-CID (spectra not shown; unpublished results) or by MALDI ion trap⁶⁰ since that would necessitate a multitude of “bridged” structures, of varying large ring size, between the single protonated arginine residue and each acidic side-chain moiety.

We argue that a different model from that proposed earlier⁵ is better suited to explain the obvious fragmentation trends that are observed for the acidic and basic residue-containing peptides. In general, this model (shown in Scheme 2) favors solvation of

Scheme 2. Model Illustrating the Intramolecular Interactions Leading to the Specific Cleavage at (A) the Seventh D Residue in **RLDIFSDFR** and (B) the Seventh C Residue in **RLAIFSC*FR** and (C) A Similar Mechanism for Cleavage at the Seventh E Residue in **RLEIFSEFR**^a



^a Due to the additional $-\text{CH}_2$ in the side chain of E, a stable eight-membered ring cannot form (or forms more slowly) in the ESI/SID experiment time frame.

the sequestered proton(s) on arginine(s) by nearby carboxylic acid groups and/or heteroatoms (e.g., carbonyl oxygens), with specific backbone cleavage(s) initiated by any free acidic hydrogen(s). Specifically for the $[\text{M} + 2\text{H}]^{2+}$ ions of **RLDIFSDFR** and **RLEIFSEFR** (Scheme 2A and 2C), one of the charges added by ionization is solvated between the guanidino side chain of the N-terminal R residue and the acidic side chain of the D or E residue at the third position, respectively, while the C-terminal protonated R residue is solvated by the carboxy terminus. Solvation of the C-terminal protonated R by the carboxy terminus involves formation of a smaller ring size than solvation by the seventh acidic residue and is thus expected to be favored over solvation by the seventh residue. This would allow the acidic proton on the D at the seventh residue to intramolecularly induce fragmentation at its C-terminal amide bond, leading to an enhanced cleavage. Thus, the formation of b_7/y_2 in the $[\text{M} + 2\text{H}]^{2+}$ ions of **RLDIFSDFR** and **RLEIFSEFR** can now occur via the mechanism proposed by Yu et al.⁸⁹ Cleavages induced by the acidic hydrogens *not solvating the protonated R residue* also explain the mass spectral results of fibrinopeptide A (enhanced cleavage is seen at each of the 2 D or 7 E) and [Glu-1] fibrinopeptide B⁶⁰ (enhanced cleavage is seen at each of the 3 D or 4 of 5 E residues), both of which have an R at the C-terminus.

Cleavage at the C^* residue in **RLAIFSC*FR** may also occur in a similar manner (Scheme 2B). It is also conceivable that the N-terminal protonated R interacts with the C^* residue at

position 7 in doubly protonated $RLAIFSC^*FR$ prior to activation but that SID or CID interrupts this interaction in the fragmenting structure, enabling C^* to initiate cleavage. This possibility can also be used to rationalize the strong y_6 product ion of doubly protonated $RLC^*IFSAFR$. However, based on the MS/MS results of doubly protonated RLC^*IFSC^*FR (spectrum not shown), facile cleavage C-terminal to the C^* at position 7 occurs in preference to the cleavage at position 3. This suggests either that the single C^* in the 7 or 3 position ($RLAIFSC^*FR$ and $RLC^*IFSAFR$, respectively) is not solvating the protonated arginine or that, in the case of RLC^*IFSC^*FR , the “free” C^* at position 7 leads to faster cleavage than cleavage at the C^* in position 3, which, if originally bridged to protonated arginine, must separate from the arginine and rearrange to allow cleavage. Computational results suggest that an interaction might exist between N-terminal protonated R and the C^* residue at position 3 or 7 (with single C^*). MP2 6-31G**/6-31G* ab initio calculations for methyl guanidine and methyl sulfonic acid show formation of two H-bonds for the interaction of the neutrals; this H-bonded structure is 80 kcal/mol more stable than a “remote” sulfonic acid anion and protonated imino group (unpublished results). A similar preference for the neutral bridged structure rather than “zwitterions” has been published for guanidino-carboxylic acid systems.^{15,94} Formation of only one H-bond (shallow minimum) is predicted when calculations are performed for the interaction of protonated methyl guanidine with methyl sulfonic acid.

Peptide fragmentation in a tandem mass spectrometer is kinetically controlled such that those processes that can be attained within the experimental time frame are sampled in preference to those that are not. In principle, the side chain of E can induce fragmentation of the C-terminal amide bond adjacent to it via formation of an eight-membered ring. However, if the experimental time frame is not sufficient for the process to occur, the product ions resulting from such a fragmentation cannot be detected. Such a kinetically slow but enhanced cleavage at E is supported by the mass spectral data of $RLAIFSEFR$ and $LEIFSEFR$, which show that this cleavage is readily observable in the long time frame afforded by SORI-CID but not in the time frame of ESI/SID (Figure 8). The proximity of the nucleophilic carboxylate oxygen to the carbonyl oxygen of the amide bond is also a potential factor in the observable preference of cleavage at D vs E during ESI/SID (Figure 7). The carboxylate oxygen of the D residue side chain (which contains one $-CH_2$ group) is expected to be more proximal to the amide oxygen than the carboxylate oxygen of a E residue side chain (which contains two $-CH_2$ groups) at the same position. Modeling of this interaction is ongoing in our laboratory in order to address this “entropy factor” further.

The model shown in Scheme 2 also supports the cleavages seen for the $[M + H]^+$ ions of $LDIFSDFR$ and $LEIFSEFR$. In these peptides, the charge on the C-terminal protonated R is solvated by the C-terminus, which allows the acidic protons on the second and sixth residues to induce cleavage. In the case of $LDIFSDFR$, bridging to the carboxylic acid at the C-terminus forms a smaller (10-membered) ring size than that necessary to bridge to the Asp side chains. Although this ring size seems large, there is a large driving force to “bury” charge in “naked” gas-phase ions. Strong y_2 and y_6 fragment ions in $[LDIFSDFR + H]^+$ and $[LEIFSEFR + H]^+$ when there is no R at the amino terminus and weak, if any, b_3 ions in $[RLDIFSDFR + 2H]^{2+}$ and $[RLAIFSEFR + 2H]^{2+}$ (which would imply cleavage at

the first acidic residue) is further supporting evidence that the N-terminal protonated R residue is interacting with the acidic residue at the third position. We hypothesize that, in the $[M + H]^+$ ions of $RLDIFSDFR$, the cleavages at both D residues are attributable to the protonated R residue being solvated by any one of the carboxylic acid groups. This would leave one of the acidic residues in the third or seventh position or both (D at position 3 and 7, with solvation at the C-terminus) to initiate a cleavage. Bridging to any carboxylic group requires a larger ring, with a 15-membered ring being the smallest possible. This could result in no bridging or, perhaps (as the mass spectral data seem to suggest), a mixture of structures with some percentage of structures solvated by each of the different carboxylic acids. Thus, multiple conformers could exist for this protonated peptide in the gas phase. Nonetheless, the excellent correspondence which is observed between spectra obtained with three different methods (keV-CID, eV-CID with long time scale, and eV-SID) suggests stable peptide structure(s) that dictates the dissociation, consistent with the model in Scheme 2. Modeling studies are underway to elucidate the conformation in the gas phase of singly protonated ions of $RLDIFSDFR$ and $LDIFSDFR$. In the absence of a highly basic site that sequesters charge ($LDIFSDFR$), the mobile proton is responsible for inducing nonselective fragmentation.

This general model (Scheme 2) can also be used to predict and explain the dissociation behavior when the number of ionizing protons is less than the number of arginine residues, as would be the case for singly protonated $RLDIFSDFR$. In such a population of singly protonated peptide ions, the ionizing proton can be sequestered at either of the two R residues. Solvation of the sequestered charge at the C-terminal R and initiation of cleavage C-terminal by the acidic hydrogens at each of the two free D residues should result in dominant y_6 and y_2 ions, similar to singly protonated $LDIFSDFR$ (Figure 5). A dominant b_7 ion is expected (similar to that for singly protonated $RLDIFSDFR$; Figure 4B) on dissociation of the population of singly protonated $RLDIFSDFR$ ions when the charge is sequestered and solvated at the N-terminal R residue (by either nearby carboxylic or amide carbonyl oxygens). The MS/MS results for the $[M + H]^+$ ions of $RLDIFSDFR$ support these predictions (spectra not shown). Further support for the model of Scheme 2 is provided by recent results in which a fixed-charge surrounded by bulky substituents (tri(2,4,6-trimethoxyphenyl)phosphonium), is covalently bound to $LDIFSDFR$. Fragmentation of this peptide leads to selective cleavage at both aspartic acids (unpublished results).

Conclusions

The existence of intraionic interactions in gas-phase peptide ions and the influence of these interactions on dissociation are supported by data obtained with three different activation methods that deposit different distributions of energy and that are associated with different time frames for dissociation. Strongly preferred cleavages adjacent to cysteic, aspartic, and glutamic acid residues in arginine-containing peptides have been observed, in agreement with previous findings of similar dominant cleavages at acidic residues.^{3,11,13,55,59,60,65,72,88–90} A model based on solvation of the “sequestered” charge on arginine by nearby carboxylic acid groups and preferential initiation of cleavage by acidic hydrogens not involved in the charge solvation has been proposed. Moreover, it is believed that this model may help explain previous observations of preferred cleavages at acidic residues, especially in peptides where basic residues are also present. The results can be

(94) Zheng, Y.-J.; Ornstein, R. L. *J. Am. Chem. Soc.* **1996**, *118*, 11237–11243.

regarded as supporting evidence for the existence of peptide secondary structure in the gas phase. The clear shifts to lower onset energies for dissociation in the peptides containing both acidic and basic residues also suggest an overriding contribution from intramolecular interactions to the energy required for fragmentation of these peptides. Moreover, this work emphasizes that certain conformations adopted by peptides in the gas phase must be limited by their rates of formation since preferred cleavages at glutamic acids are observed only in the long time frame afforded by SORI–CID in an FTMS but not by SID in a quadrupole tandem mass spectrometer. Hence, a systematic and thorough approach including different dissociation time frames and methods of energy deposition should always be taken when probing for evidence of peptide gas-phase structure.

Finally, evidence in support of a mobile proton when the number of ionizing protons exceeds the number of basic sites has also been demonstrated by this work. The mobile proton model^{37,38} is also applicable for peptides containing acidic residues only. We are currently pursuing ways to refine this model for dominant cleavages at acidic residues in the presence of basic residues, as well as gathering further support for conformation and structure of peptides in the gas phase. It is hoped that such mechanistic information will be used to improve automated sequence strategies.

Acknowledgment. This work was financially supported by a grant from the National Institutes of Health (GM51387 to V.H.W), the National Science Foundation (CHE-9616711 to J.H.F), and U.K. EPSRC (GR/K18658 to S.J.G.). We also thank Dr. Eugene Nikolaev for his help with some of the high-energy CID spectra and Ricardo Gonzalez for preparing some of the figures for this manuscript.

Supporting Information Available: ESI/SID spectra of $[M + 2H]^{2+}$ ions of RLCIFSAFR (55 eV), RLC*IFSAFR (55 eV), RLCIFSCFR (55 eV), RLC*IFSC*FR (55 eV), RLCIFSAFR (80 eV); SORI–CID (17 eV) and high-energy CID (~ 10 keV) spectra of $[M + H]^+$ ions of LDIFSDF; ESI/SID spectra of $[M + 2H]^{2+}$ ions of LDIFSDFR (25 eV) and RLDIFSDF (40 eV); SORI–CID spectra of $[M + 2H]^{2+}$ ions of LDIFSDFR (15.5 eV) and RLDIFSDF (12 eV); high-energy CID (~ 10 keV) spectra of $[M + 2H]^{2+}$ ions of RLDIFSDF and LDIFSDFR; SORI–CID spectra of $[M + H]^+$ ions and $[M + 2H]^{2+}$ ions of LEIFSEFR both at 15 eV; and ESI-LCQ spectrum of $[M + H]^+$ ions of RLDIFSDFR as well as MS³ spectrum of the y_6 product ion (PDF). This material is available free of charge via the Internet at <http://pubs.acs.org>.

JA982980H